Quantum-enhanced continuous-wave stimulated Raman scattering spectroscopy

de Andrade, Rayssa B.; Kerdoncuff, Hugo; Berg-Sørensen, Kirstine; Gehring, Tobias; Lassen, Mikael Østergaard; Andersen, Ulrik L.

Published in:
Optica

Link to article, DOI:
10.1364/OPTICA.386584

Publication date:
2020

Document Version
Publisher's PDF, also known as Version of record

optica

Quantum-enhanced continuous-wave stimulated Raman scattering spectroscopy

Rayssa B. de Andrade,[1,*] Hugo Kerdoncuff,[2] Kirstine Berg-Sørensen,[1] Tobias Gehring,[1] Mikael Lassen,[2] and Ulrik L. Andersen[1]

[1]Center for Macroscopic Quantum States bigQ, Department of Physics, Technical University of Denmark, Fysikvej 307, DK-2800 Kgs. Lyngby, Denmark
[2]Danish Fundamental Metrology, Kogle Alle 5, DK-2970 Hørsholm, Denmark
*Corresponding author: rabda@fysik.dtu.dk

Received 23 December 2019; revised 8 April 2020; accepted 10 April 2020 (Doc. ID 386584); published 7 May 2020

Stimulated Raman spectroscopy has become a powerful tool to study the spatiodynamics of molecular bonds with high sensitivity, resolution, and speed. However, the sensitivity and speed of state-of-the-art stimulated Raman scattering spectroscopy are currently limited by the shot-noise of the light beam probing the Raman process. Here, we demonstrate in a proof-of-principle experiment an enhancement of the sensitivity of continuous-wave stimulated Raman spectroscopy by reducing the quantum noise of the probing light below the shot-noise limit by means of amplitude squeezed states of light. Probing polymer samples with Raman shifts around 2950 cm^{-1} with squeezed states, we demonstrate a quantum enhancement of the stimulated Raman signal-to-noise ratio (SNR) of 3.60 dB relative to the shot-noise limited SNR. Our proof-of-concept demonstration of quantum-enhanced continuous-wave Raman spectroscopy paves the way for more elaborate demonstrations using state-of-the-art stimulated Raman scattering microscopes, and thus constitutes the very first step towards a new generation of Raman microscopes, where weak Raman transitions can be imaged without the use of markers or an increase in the total optical power.

https://doi.org/10.1364/OPTICA.386584

1. INTRODUCTION

Optical quantum sensing exploits the unique quantum correlations of non-classical light to enhance the detection of physical parameters beyond classical means [1–5]. While several different quantum states of light can, in principle, be used to provide such a quantum advantage, so far, it is only the ubiquitous squeezed states of light that have demonstrably been shown to provide a real practical advantage [6–8] due to its generation simplicity and robustness to loss. Squeezed states of light have, for example, enabled quantum-enhanced measurements of mechanical displacements [5,9], magnetic fields [10,11], viscous elasticity of cells [12], and, most prominently, gravitational waves [13]. Another field that could significantly benefit from quantum-enhanced sensing by means of squeezed light—but not yet demonstrated—is Stimulated Raman Scattering (SRS) spectroscopy.

SRS spectroscopy is a very powerful technique to perform real-time vibrational imaging of living cells and organisms, and it has therefore provided a deeper understanding of properties of biological systems [14–17]. It is based on the stimulated excitation of a Raman transition of the sample under interrogation, thereby resulting in a measurable stimulated Raman loss and gain of the two input beams. It allows for non-invasive and *in vivo* measurements with short acquisition times [18], and has enabled the structural and dynamical imaging of lipids [19,20] as well as the characterization of healthy and tumorous brain tissues [21,22].

In SRS, the sensitivity and imaging speed are fundamentally limited by the noise level (often shot-noise) of the probing laser [23,24], but can in principle be arbitrarily improved by simply increasing the power of the input beams. However, in biological systems, especially in living systems, the power must be kept low to avoid changing the biological dynamics of the specimens, and in particular to avoid damage due to excessive heating. Leaving the optical power at a constant level, the sensitivity and bandwidth of the SRS can be boosted by reducing the shot-noise level using squeezed states of light.

In this paper, we demonstrate the quantum enhancement of continuous-wave (cw) SRS spectroscopy using amplitude squeezed light. We demonstrate its functionality and superiority by spectroscopically measuring the carbon–hydrogen (C-H) vibrations of polymethylmethacrylate (PMMA) and polydimethylsiloxane (PDMS) with a sensitivity improvement of approximately 56% relative to shot-noise limited Raman spectroscopy. Our measurement method has the potential to enable new measurement regimes of Raman bioimaging that are inaccessible by conventional shot-noise limited Raman spectroscopy.

2. BASIC CONCEPT

SRS employs two laser beams, known as the pump and probe (Stokes) beams, to coherently excite a selected molecular vibration of the system under investigation. If the vibrational frequency of the chemical bond matches the frequency difference of the pump and probe laser, the Raman interaction is stimulated and, as a result, significantly amplified by orders of magnitude. In the stimulated Raman effect, a photon is annihilated from the pump beam and, simultaneously, a Raman-shifted photon is created in the background noise of the probe beam. The intensity of the scattered light into the probe beam is

$$I_{\mathrm{SRS}} = K N \sigma I_p I_s, \tag{1}$$

where $I_{p(s)}$ is the intensity of the pump (probe) beam, N is the number of probed molecules, σ is the Raman cross section, and K is a constant that depends on the system [25]. In order to detect the stimulated scattering of photons from pump to probe, a modulation scheme is often employed. An intensity modulation is applied to one of the two beams and gets transferred to the other beam by SRS. The resulting modulation is detected with an intensity detector and lock-in amplifier at a sideband with a frequency ω_L. High-frequency modulation is often used to achieve shot-noise limited detection.

The precision by which the Raman signal can be measured depends on the background noise of the probe beam. This background noise is fundamentally limited by shot-noise when the probe beam is in a coherent state produced by a conventional laser, but it can be reduced by the use of a squeezed state. By employing a bright amplitude squeezed beam (squeezed state with a large coherent excitation described as $I_s\delta(\omega) + \sqrt{I_s}\delta X_s(\omega)$, where $\delta(\omega)$ is the Kronecker delta at the frequency ω and δX_s represents the coherent excitation and quadrature fluctuations, respectively), the power density of the detected beam is

$$\langle I^2(\omega)\rangle = I_s^2\delta(\omega) + I_s\langle X_s^2(\omega)\rangle + K^2N^2\sigma^2 I_p^2 I_s^2\delta(\omega-\omega_L), \tag{2}$$

where $\langle X_s^2(\omega)\rangle$ is the squeezing spectrum. The signal-to-noise ratio is

$$\mathrm{SNR} = \frac{K N \sigma I_p I_s}{\sqrt{I_s\langle X_s^2\rangle}}, \tag{3}$$

while the minimum number of detectable molecules (the sensitivity) is

$$\delta N = \frac{\sqrt{\langle X_s^2\rangle}}{K\sigma I_p\sqrt{I_s}}. \tag{4}$$

It is thus clear that the sensitivity can be improved without changing the power of the two laser beams by reducing the noise of the amplitude quadrature of the probe beam.

3. EXPERIMENTAL SETUP

The experimental setup is shown in Fig. 1. It consists of two modules: the bright squeezed light module and the SRS module, as will now be discussed in detail.

A. Bright Squeezed Light Module

The laser source was an Innolight GmbH Diabolo operating at 1064 nm with an internal module for second-harmonic generation (SHG) at 532 nm. The squeezed state was generated in a linear optical parametric oscillator (OPO) cavity consisting of a periodically poled potassium titanyl phosphate (PPKTP) crystal and a hemispheric coupling mirror. When pumping with a power of 80 mW at 532 nm, setting the phase of the pump beam to deamplification and injecting a seed beam with a power of 600 μW at 1064 nm, the OPO produced 7 dB of amplitude squeezed light. More details about the squeezed light source can be found in Ref. [26]. The amplitude squeezed light and a coherent beam at 1064 nm were combined on an asymmetric (99/1) beam splitter to produce a bright amplitude squeezed beam. The phase between these beams was actively stabilized by feeding a phase shifter in the coherent beam path with an error signal that was generated by electronically demodulating the photodetected beat of the bright coherent beam and the 37.22 MHz phase modulation side-bands accompanying the squeezed field. The output of the 99% port of the BS was sent to the SRS module serving as the probe beam for Raman spectroscopy.

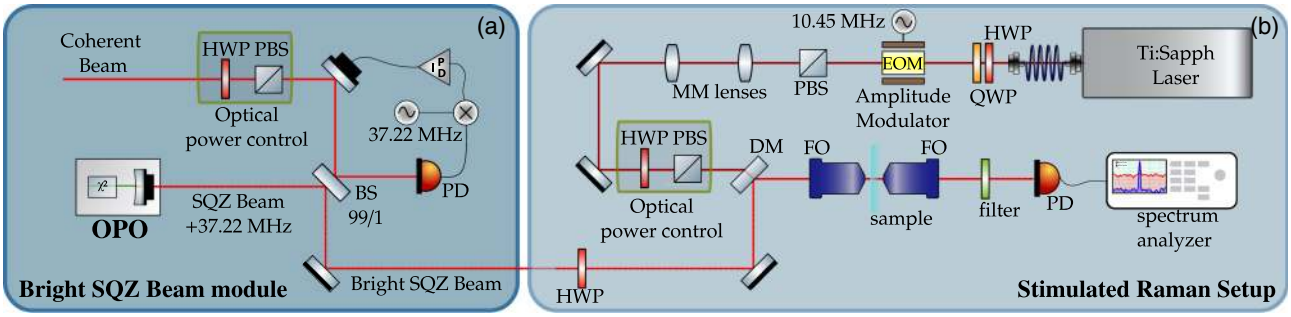

Fig. 1. Experimental setup to measure the SRS signal enhanced by squeezed light. (a) Bright squeezed beam preparation at 1064 nm. The squeezed state is combined with the coherent beam in a 99/1 beam splitter (BS) to generate a bright squeezed state at one output serving as the probe for the SRS setup, while the other output is used to phase-lock the relative phase of the two beams (using a phase modulation at 37.22 MHz). (b) SRS setup. A wavelength-tunable Ti:Sapphire laser is intensity modulated at the frequency of 10.45 MHz and serve as the pump beam. The pump and probe beams are overlapped in a dichroic mirror (DM) and focused into the sample using a microscope objective (FO). The SRS signal is collected using a second objective; the pump beam is filtered off and the probe beam is measured using a high-quantum-efficiency (HQE) photodiode. The results are acquired by an electronic spectrum analyzer (ESA) by which a power spectrum of the signal is attained. HWP, half wave plate; PBS, polarizing beam splitter; PD, photodiode; BS, beam splitter; QWP, quarter-wave plate; DM, dichroic mirror; FO, focal objective; EOM, electro-optical modulator; MM lenses, mode-matching lenses.

B. Stimulated Raman Module

The pump beam for SRS spectroscopy was a tunable Ti:Sapphire laser (MSquare SolsTiS) scanned from 800 to 830 nm. It delivered a maximum output power of 200 mW which could be adjusted at the entrance to the microscope. The pump beam intensity was modulated at 10.45 MHz with a sinusoidal function using a resonant electro-optical amplitude modulator. The beam size of the pump beam was adjusted with a set of lenses (MM lenses) in order to optimize the overlap with the probe beam. A fine adjustment in the polarization between the pump and probe beams was made using a HWP (half-wave plate) in the probe path. After combining the probe and pump beams at a dichroic mirror, both beams were focused to a spot size of 2.5 μm on the sample with a 20x microscope objective. The beams were collected and collimated by a second microscope objective, after which the pump beam was filtered using a long-pass filter and the probe beam was detected using a photodiode with a quantum efficiency of more than 99% (Fermionics InGaAs FD500). The stimulated Raman gain was deduced from the power spectrum, which was recorded using an electrical spectrum analyzer.

Important factors when using squeezed light are the optical losses in the optical pathway of the squeezed beam. From the output of the OPO cavity to the entrance of the microscope, we estimated an overall optical efficiency of around $\eta_{\text{path}} = 85\%$, while each of the two microscope objectives had a transmission efficiency of 97%. The visibility between the coherent and squeezed beams was 95%. Thus, the total efficiency transmission of the 1064 nm path, including also the detection losses, was estimated to $\eta_{\text{total}} = 67\%$.

In this work, we use two different solid samples to characterize the SRS spectroscopy process, PMMA and PDMS. Both samples have Raman transitions in the region between $2800-3100\ \text{cm}^{-1}$ corresponding to vibration modes of the C-H bonds [27,28]. We start by classically characterizing the Raman transition of a PMMA sample of 2 mm thickness and a pump laser with a power at the sample of 38 mW, tuned to the wavelength of 810.241 nm to hit the Raman transition at $2948.32\ \text{cm}^{-1}$. The SRS signal was measured on the probe beam (due to the stimulated gain) at the modulation frequency of the pump at 10.45 MHz, and we acquired a power spectrum around this frequency. In absence of the SRS signal, only measurement noise was detected. The data presented have all been measured using a resolution bandwidth of 30 Hz and a video bandwidth of 1 Hz; each data point was averaged 30 times, and the electronic noise was subtracted in all the measurements. The probe power was changed from 250 μW to 2.0 mW, as shown in Fig. 2(a), and we clearly observe the expected linear dependency between SRS signal and probe power. The polarization behavior between pump and probe beams are shown in Fig. 2(b), where the red trace represents the signal when the pump and probe beams were parallel polarized while the blue trace corresponds to the signal when the beams were orthogonal polarized. It is clear that the Raman signal disappears in the latter case, thus further corroborating the presence of real Raman signal in the former case [29,30]. Both traces were normalized by the shot-noise.

Having verified the C-H Raman transition, in the following, we present the demonstration of quantum-enhanced SRS spectroscopy. To clearly demonstrate quantum-improved performance beyond the conventional approach, we conducted the experiment both with the probe beam in a coherent state (limited by shot-noise and representing the conventional approach) and in the squeezed state. The experimental scheme could easily be swapped between the two modes of operation simply by blocking and unblocking the squeezed vacuum state, which will have no effect on the probe or pump input powers.

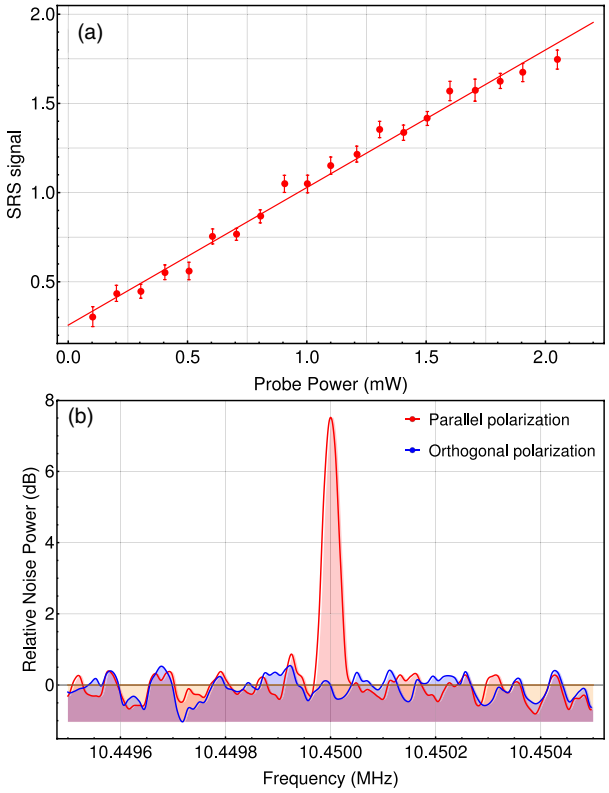

Fig. 2. Characterization of the SRS signal using an average pump power of 38 mW. (a) Intensity of the SRS signal as a function of the probe power. (b) Polarization behavior of the SRS signal using 1.35 mW of power in the probe beam. The red trace represents the signal when the probe and pump beams are parallel polarized, while the blue trace is associated with orthogonal polarized beams. All traces are normalized to the shot-noise level.

4. EXPERIMENTAL RESULTS

Figure 3 presents our experimental results for quantum-enhanced SRS spectroscopy. We present the spectra for the Raman shift of PMMA using both a coherent state (for comparison) and a squeezed state with optical powers of 1.3 mW while the pump power was set to 24 mW [Fig. 3(a)] and 11 mW [Fig. 3(b)]. It is clear from the spectra that the usage of squeezed light significantly improves the signal-to-noise ratio, and therefore the sensitivity of the Raman spectrometer. We see in particular that for pump powers lower than around 11 mW, the Raman signal is almost embedded in shot-noise and only becomes pronounced when using squeezed states of light. It is therefore clear that by using the quantum-enhanced operation mode, it is possible to attain Raman signals even for low pump powers. This is of importance when studying fragile biological systems where excessive powers might change the dynamics of the system.

In Fig. 4, we plot the SNR for the PMMA vibrational mode as a function of the power of the pump beam both for the case where the Stokes beam is prepared in a coherent state and in a squeezed

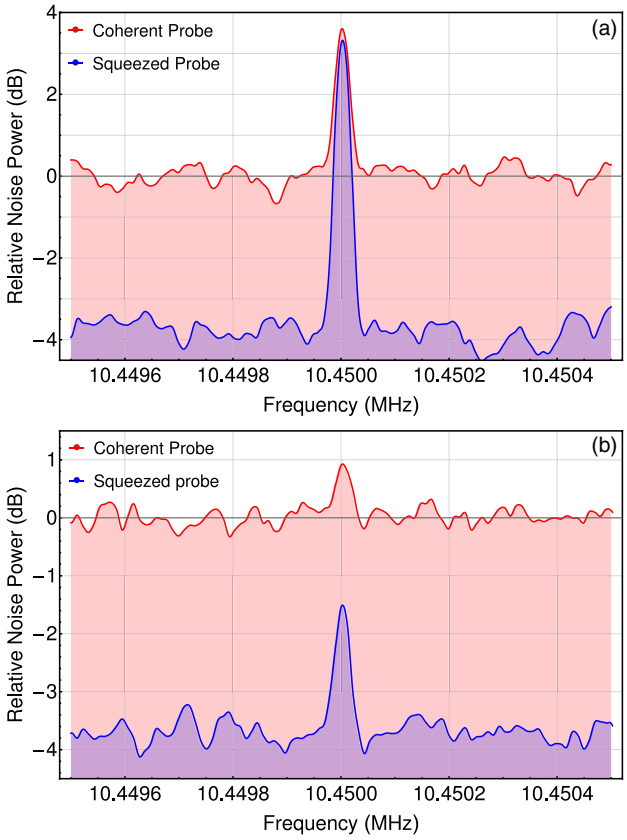

Fig. 3. Demonstration of quantum enhanced SRS spectroscopy using probe powers of 1.3 mW and pump powers of (a) 24 mW and (b) 11 mW. The red SRS traces correspond to the realizations where the probe beams are in a coherent state while the blue traces correspond to the beams being in a squeezed state with −3.60 dB noise suppression below the shot-noise. In both cases, the signals are normalized to the shot-noise level.

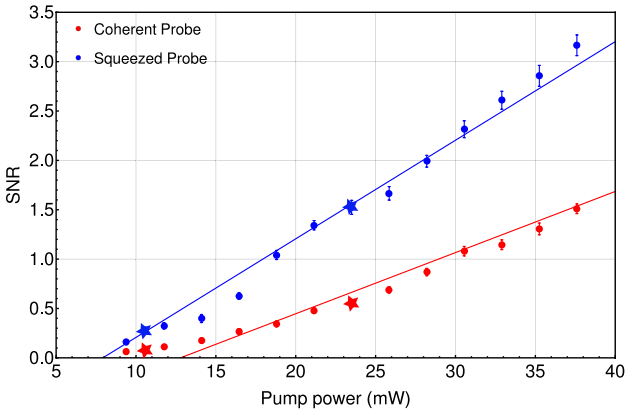

Fig. 4. Linear dependence of the SNR in terms of the pump power for the PMMA vibrational mode at 2948.75 cm^{-1}. The red data points and theoretically estimated line correspond to the probe beam being in a coherent state, while the blue points and line correspond to the beam being in a squeezed state. The realizations illustrated in Fig. 3 are marked by stars.

state. We fit the theoretical prediction [Eq. (3)] to the experimental data points and attain the expected linear relationship between SNR and pump power. The effect of squeezing is to increase the slope of this relationship as clearly seen from the plots.

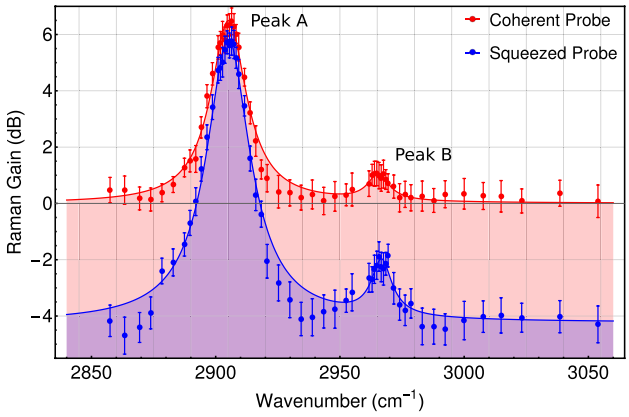

Fig. 5. SRS spectrum of PDMS. The pump beam is scanned around the C-H stretching region with pump and probe powers of 28 and 1.3 mW, respectively. The traces are normalized to the shot-noise level.

The SRS spectroscopy process provides a Raman spectrum similar to the spectrum generated using spontaneous Raman spectroscopy techniques. Using a PDMS sample and sweeping the pump laser manually from 803.36 to 816.36 nm, the Raman spectrum of the C-H stretching modes in the region between $2850 - 3100\ cm^{-1}$ was acquired and is depicted in Fig. 5. The probe and pump optical powers were 1.3 and 28 mW, respectively. While scanning the wavelength of the pump laser, the optical pump power was continuously measured and used to normalize the acquired Raman spectrum at every wavelength. In Fig. 5, the spectra are shown for coherent (red trace) and squeezed states (blue trace). Lorentzian multipeak fits were used to obtain the two Raman shifts in Table 1.

As a next step, we measured Raman signals spatially distributed in a sample consisting of three different polymers; PMMA, PDMS, and polystyrene. A three-axes translational stage with differential micrometer screws was used to move, manually, the sample position in steps of 1 mm in a square region of $7 \times 7\ mm^2$. The SRS signal was acquired using coherent and squeezed states of light alternately for each displacement. Applying an average pump power of 28 mW and a probe power of 1.3 mW, the pump laser wavelength is set up to 810.213 nm corresponding to a Raman shift 2948.75 cm^{-1}, and the PMMA content in the sample was detected. Figure 6(a) shows the result. Afterwards, to detect the PDMS content in the sample, the pump wavelength was changed to 813.111 nm, corresponding to the vibrational mode 2904.76 cm^{-1}. The result is shown in Fig. 6(b). The remaining area comprising polystyrene exhibits no signals, as it has no vibrational modes in the interrogated frequency region.

We clearly see from the figure that PMMA and PDMS can be distinguished with the method, and we also find that squeezed light outperforms coherent light operation in the entire plane. These spatially distributed quantum-enhanced Raman measurements represent the very first steps towards quantum-enhanced Raman microscopy, which will be the next natural step to demonstrate quantum superiority in imaging. This is an alternative to quantum-enhanced microscopes based on interferometry using NOON states [31] or photon number correlated states [32]. As an outlook, the quantum-enhanced technique should be implemented in a state-of-the-art Raman microscope to go beyond what is currently reachable with classical technology.

Table 1. Raman Resonances of PDMS: Peak A and Peak B[a]

Probe Beam	Assignment	$\nu_{\mathrm{PeakA}}\,(\mathrm{cm}^{-1})$	SNR_A (dB)	$\nu_{\mathrm{PeakB}}\,(\mathrm{cm}^{-1})$	SNR_B (dB)
Coherent light	C-H sym	2905.17 (0.15)	6.49 (0.08)	2965.46 (1.17)	0.95 (0.18)
Ampl. squeezed light	C-H sym	2905.07 (0.14)	10.05 (0.07)	2966.74 (0.80)	2.01 (0.18)

[a]The Raman shifts are represented as ν_{PeakA} and ν_{PeakB}.

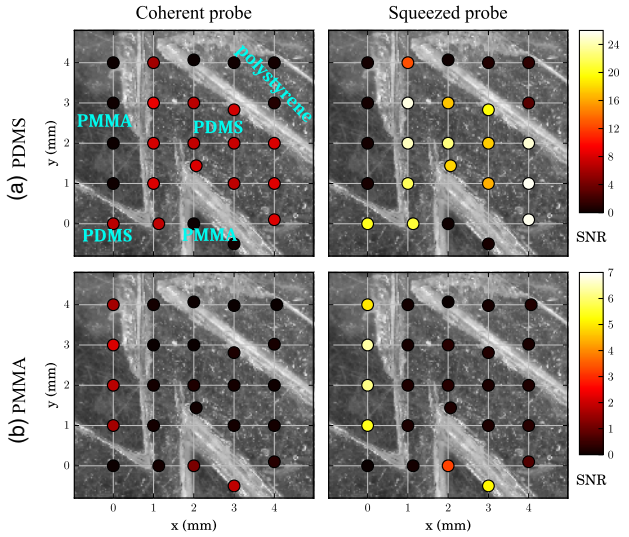

Fig. 6. SRS spatially distributed Raman measurements of different polymers in a sample comprising PDMS, PMMA, and polystyrene using coherent (left side) and squeezed (right side) probe beams. (a) Measurements of the SNR attained when the pump laser frequency was set to reach the PDMS vibrational mode 2904.76 cm^{-1} and (b) the vibrational mode 2948.75 cm^{-1} of PMMA. The remaining area (polystyrene) does not produce an SRS signal. The gray areas in the background are optical microscope images of the sample. In (a), we denote the material system with blue font.

While our quantum-enhanced Raman spectroscopy demonstration is based on cw laser beams, it is important to mention that state-of-the-art high-sensitivity Raman spectrometers are based on strongly focused pico- or femtosecond pulsed lasers with very high peak powers [19,33]. Pulsed SRS microscopes attain sensitivities that are orders of magnitude larger [34] than cw SRS microscopes but, due to the large peak powers, they cannot necessarily be applied when interrogating fragile light- and heat-sensitive biological specimens. For these particular applications, the squeezing-enhanced cw Raman spectrometer will be the natural choice as, on the one hand, cw laser beams are less damaging and on the other hand, squeezed light improves the SNR without increasing the power. However, to beat the performance of current state-of-the-art SRS microscopes by means of squeezed light, one must employ squeezed picosecond pulses in a strongly focusing configuration (using an objective with a numerical aperture above unity).

5. CONCLUSION

In summary, we have demonstrated a sensitivity enhancement of the SRS spectroscopy process using squeezed states of light. The quantum enhancement was measured to be more than 50% in comparison to the conventional approach with coherent states. Our technique was used to visualize spectroscopically the Raman bands within the C-H stretching region of polymer samples (PMMA and PDMS) and to perform chemically specific imaging measurements. The sensitivity of our quantum spectrometer can be further improved by minimizing the optical losses of the system and employing states with a higher degree of squeezing. Moreover, to realize real and high-resolution SRS imaging, the sample should be scanned with high spatial resolution, and the objectives replaced with ones having higher numerical apertures.

We believe that our demonstration opens the door to new possibilities for SRS spectroscopy and microscopy. Using squeezed light to enhance the sensitivity of the stimulated Raman signal enables studies of biological samples with a lower risk of damage due to high beam powers. This might enable the study of biophysical effects that may not be visible using the standard classical approaches. The presented method is not limited to the wavenumber range investigated in this work, but can be extended to the fingerprint region ($500 - 1800\,\mathrm{cm}^{-1}$) by appropriate choice of laser wavelengths, thereby giving access to detailed information and the rich dynamics of different biological samples.

Funding. Danmarks Grundforskningsfond (DNFR412); Innovationsfonden (Qubiz); European Metrology Programme for Innovation and Research (17FUN01-BeCOMe); Danish Agency for Institutions and Educational Grants.

Disclosures. The authors declare no conflicts of interest.

REFERENCES

1. B. J. Lawrie, P. D. Lett, A. M. Marino, and R. C. Pooser, "Quantum sensing with squeezed light," ACS Photon. **6**, 1307–1318 (2019).
2. S. Pirandola, B. R. Bardhan, T. Gehring, C. Weedbrook, and S. Lloyd, "Advances in photonic quantum sensing," Nat. Photonics **12**, 724–733 (2018).
3. K. Marshall, C. S. Jacobsen, C. Schäfermeier, T. Gehring, C. Weedbrook, and U. L. Andersen, "Continuous-variable quantum computing on encrypted data," Nat. Commun. **7**, 13795 (2016).
4. M. A. Taylor and W. P. Bowen, "Quantum metrology and its application in biology," Phys. Rep. **615**, 1–59 (2016).
5. U. B. Hoff, G. I. Harris, L. S. Madsen, H. Kerdoncuff, M. Lassen, B. M. Nielsen, W. P. Bowen, and U. L. Andersen, "Quantum-enhanced micromechanical displacement sensitivity," Opt. Lett. **38**, 1413–1415 (2013).
6. A. I. Lvovsky, "Squeezed light," in *Photonics*, D. L. Andrews, ed. (Wiley, 2015), Chap. 5, pp. 121–163.
7. U. L. Andersen, T. Gehring, C. Marquardt, and G. Leuchs, "30 years of squeezed light generation," Phys. Scripta **91**, 053001 (2016).
8. R. Schnabel, "Squeezed states of light and their applications in laser interferometers," Phys. Rep. **684**, 1–51 (2017).
9. R. C. Pooser and B. Lawrie, "Ultrasensitive measurement of microcantilever displacement below the shot-noise limit," Optica **2**, 393–399 (2015).
10. F. Wolfgramm, A. Cerè, F. A. Beduini, A. Predojević, M. Koschorreck, and M. W. Mitchell, "Squeezed-light optical magnetometry," Phys. Rev. Lett. **105**, 053601 (2010).
11. B.-B. Li, J. Bílek, U. B. Hoff, L. S. Madsen, S. Forstner, V. Prakash, C. Schäfermeier, T. Gehring, W. P. Bowen, and U. L. Andersen, "Quantum enhanced optomechanical magnetometry," Optica **5**, 850–856 (2018).

12. M. A. Taylor, J. Janousek, V. Daria, J. Knittel, B. Hage, H.-A. Bachor, and W. P. Bowen, "Biological measurement beyond the quantum limit," Nat. Photonics **7**, 229–233 (2013).
13. T. L. S. Collaboration, "Enhanced sensitivity of the LIGO gravitational wave detector by using squeezed states of light," Nat. Photonics **7**, 613–619 (2013).
14. C. W. Freudiger, W. Yang, G. R. Holtom, N. Peyghambarian, X. S. Xie, and K. Q. Kieu, "Stimulated Raman scattering microscopy with a robust fibre laser source," Nat. Photonics **8**, 153–159 (2014).
15. C. H. Camp and M. T. Cicerone, "Chemically sensitive bioimaging with coherent Raman scattering," Nat. Photonics **9**, 295–305 (2015).
16. J. X. Cheng and X. S. Xie, *Coherent Raman Scattering Microscopy*, 1st ed. (CRC Press, 2016).
17. R. R. Jones, D. C. Hooper, L. Zhang, D. Wolverson, and V. K. Valev, "Raman techniques: fundamentals and frontiers," Nanoscale Res. Lett. **14**, 231 (2019).
18. H. J. Lee and J.-X. Cheng, "Imaging chemistry inside living cells by stimulated Raman scattering microscopy," Methods **128**, 119–128 (2017).
19. W. Dou, D. Zhang, Y. Jung, J.-X. Cheng, and D. Umulis, "Label-free imaging of lipid-droplet intracellular motion in early drosophila embryos using femtosecond-stimulated Raman loss microscopy," Biophys. J. **102**, 1666–1675 (2012).
20. M. C. Wang, W. Min, C. W. Freudiger, G. Ruvkun, and X. S. Xie, "RNAi screening for fat regulatory genes with SRS microscopy," Nat. Methods **8**, 135–138 (2011).
21. M. Ji, D. A. Orringer, C. W. Freudiger, S. Ramkissoon, X. Liu, D. Lau, A. J. Golby, I. Norton, M. Hayashi, N. Y. R. Agar, G. S. Young, C. Spino, S. Santagata, S. Camelo-Piragua, K. L. Ligon, O. Sagher, and X. S. Xie, "Rapid, label-free detection of brain tumors with stimulated Raman scattering microscopy," Sci. Trans. Med. **5**, 201ra119 (2013).
22. F.-K. Lu, D. Calligaris, O. I. Olubiyi, I. Norton, W. Yang, S. Santagata, X. S. Xie, A. J. Golby, and N. Y. Agar, "Label-free neurosurgical pathology with stimulated Raman imaging," Cancer Res. **76**, 3451–3462 (2016).
23. M. Moester, F. Ariese, and J. de Boer, "Optimized signal-to-noise ratio with shot noise limited detection in stimulated Raman scattering microscopy," J. Eur. Opt. Soc. Rapid Publ. **10**, 15022 (2015).
24. H. Kerdoncuff, M. Lassen, and J. C. Petersen, "Continuous-wave coherent Raman spectroscopy for improving the accuracy of Raman shifts," Opt. Lett. **44**, 5057–5060 (2019).
25. R. W. Boyd, *Nonlinear Optics* (Academic, 2008).
26. C. Schäfermeier, M. Ježek, L. S. Madsen, T. Gehring, and U. L. Andersen, "Deterministic phase measurements exhibiting super-sensitivity and super-resolution," Optica **5**, 60–64 (2018).
27. S. Dirlikov and J. L. Koenig, "Carbon-hydrogen stretching and bending vibrations in the Raman spectra of poly (methylmethacrylate)," J. Raman Spectrosc. **9**, 150–154 (1980).
28. A. L. Smith and D. R. Anderson, "Vibrational spectra of Me_2SiCl_2, Me_3SiCl, $Me_3SiOSiMe_3$, $(Me_2SiO)_3$, $(Me_2SiO)_4$, $(Me_2SiO)_x$, and their deuterated analogs," Appl. Spectrosc. **38**, 822–834 (1984).
29. M. Tanaka and R. J. Young, "Review polarised Raman spectroscopy for the study of molecular orientation distributions in polymers," J. Mater. Sci. **41**, 963–991 (2006).
30. H. Kerdoncuff, M. R. Pollard, P. G. Westergaard, J. C. Petersen, and M. Lassen, "Compact and versatile laser system for polarization-sensitive stimulated Raman spectroscopy," Opt. Express **25**, 5618–5625 (2017).
31. T. Ono, R. Okamoto, and S. Takeuchi, "An entanglement-enhanced microscope," Nat. Commun. **4**, 2426 (2013).
32. R. Tenne, U. Rossman, B. Rephael, Y. Israel, A. Krupinski-Ptaszek, R. Lapkiewicz, Y. Silberberg, and D. Oron, "Super-resolution enhancement by quantum image scanning microscopy," Nat. Photonics **4**, 116–122 (2019).
33. B. G. Saar, C. W. Freudiger, J. Reichman, C. M. Stanley, G. R. Holtom, and X. S. Xie, "Video-rate molecular imaging in vivo with stimulated Raman scattering," Science **330**, 1368–1370 (2010).
34. C.-R. Hu, M. N. Slipchenko, P. Wang, P. Wang, J. D. Lin, G. Simpson, B. Hu, and J.-X. Cheng, "Stimulated Raman scattering imaging by continuous-wave laser excitation," Opt. Lett. **38**, 1479–1481 (2013).